Monitoring of Alpine Snow Conditions Using C-Band SAR

CLAUDIO NAVACCHI[1], BERNHARD BAUER-MARSCHALLINGER[1] & WOLFGANG WAGNER[1]

Abstract: Information about the state of a snow pack is valuable in many geoscientific applications, e.g., for hydrological run-off models. This study aimed to retrieve such information by linking C-band Sentinel-1 Synthetic Aperture Radar (SAR) data with snow profile measurements in an alpine region. A new technique for normalising the Sentinel-1 backscatter measurements was developed, accounting for the varying observation geometry. With this, a strong relationship between radar backscatter and snow wetness could be established. Moreover, the normalisation method allows to deduce snow parameter information even without well-known change detection techniques, since systematic observation effects cancel out. Using these findings for wet snow mapping, a good agreement with optical imagery could be achieved.

1 Introduction

Aperture synthesis in radar imaging enables the acquisition of high-resolution Earth observation imagery at microwave frequencies (MOREIRA et al. 2013). Most Synthetic Aperture Radar (SAR) systems operate in the microwave C-band (4-8 GHz), which exhibits a significant sensitivity to water, one of the most abundant molecules on Earth. It has proven to be an indispensable way of monitoring processes taking place within the cryosphere, e.g. iceberg monitoring and wet snow extent mapping (POWER et al. 2001, NAGLER & ROTT 2000). Thanks to the recently much improved availability of data from SAR missions and ground based snow observations in terms of spatial and temporal resolution, the relationship between high-resolution SAR backscatter data and snow properties can be studied with unprecedented quality and details.

The aim of this study was to compare snow profile measurements (e.g., snow height, grain size, snow wetness, …) collected by the *Lawinenwarndienst Tirol* with Sentinel-1 SAR time series. The major hurdle when comparing these two data sources is the pronounced impact of the topography on the Sentinel-1 measurements. Thus, before snow properties can be derived from dense Sentinel-1 time series, representations of backscatter data need to be identified that minimise the impact of orbit geometry and local topography.

This paper starts with an introduction into the state of the art in snow-backscatter modelling and common approaches for radar backscatter normalisation in Section 2. Subsequently, a short overview of the data sets serving as an input for this research is provided. In Section 4, the methodology for preparing and normalising backscatter data to enhance its comparability with respect to snow parameter measurements is described. Finally, obtained results are discussed and the paper concludes with an outlook to future research topics.

[1] TU Wien, Department of Geodesy and Geoinformation, Microwave Remote Sensing Research Group, Wiedner Hauptstraße 8, A-1040 Wien,
E-Mail: [claudio.navacchi, bernhard.bauer-marschallinger, wolfgang.wagner]@geo.tuwien.ac.at

2 State of the Art

2.1 Snow-Backscatter Modelling

In microwave remote sensing the interaction of the microwave pulses with the land surface is most commonly modelled using radiative transfer theory. This theory is very complex in the presence of a dense medium as it is the case for an aged snow pack with larger grains, fluid retention and differing layers (cf. Fig. 1).

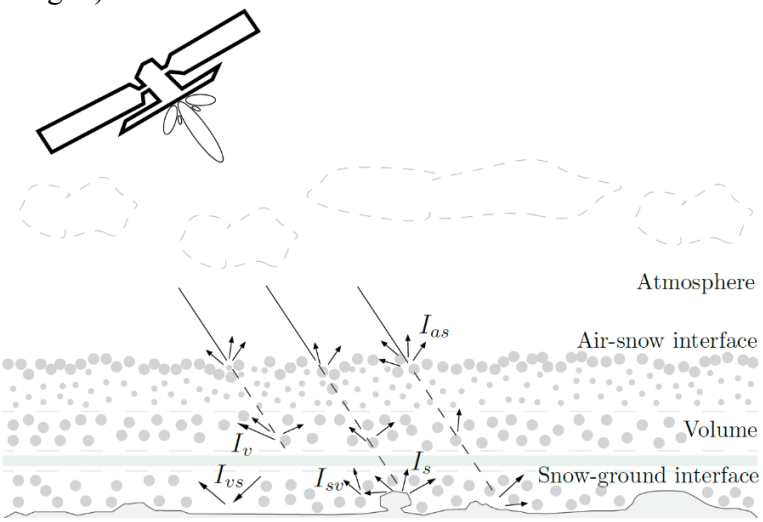

Fig. 1: Interaction of microwave radiation with a multi-layered snow pack

Yet, assumptions about the composition of the snow pack or the propagation characteristics of the radiation allow to derive certain snow parameters. This has been shown in past studies, e.g. an estimation of grain size, snow density and snow depth using the polarimetric properties of SIR-C's X/C-band sensor (SHI & DOZIER 2000), or deriving the snow water equivalence (SWE) from C-band SAR backscatter data (BERNIER & FORTIN 1998). Mapping extents of a wet snow pack is of high relevance in literature primarily being iniated by NAGLER & ROTT (2000). Until recently, change detection with an empirically defined threshold of -3 dB between wet and dry snow persisted as a suitable method for accomplishing this task (NAGLER et al. 2016). It relies on the fact, that dry snow is nearly a transparent medium at C-band frequencies, while wet snow absorbs the microwaves very quickly. Thus, the presence of wet snow, causing scattering at the air-snow interface, can be revealed by choosing a reference image at dry snow or snow-free conditions.

2.2 Radar Backscatter Normalisation

Radar backscatter normalisation is about the elimination of the dependency of backscatter on incidence angles. Diverse remote sensing satellite systems collecting multi-angle data made it possible to apply data-driven normalisation techniques. Some of those techniques rely on a high temporal resolution or a special measurement configuration. Scatterometers, such as ERS-SCAT or ASCAT, allow for a direct (i.e. in one overpass) normalisation, since the same area is measured almost simultaneously with multiple beams under different observation angles (NAEMI et al. 2009). For other sensors like ASAR on ENVISAT, dense backscatter and incidence angle time series data is used to estimate a slope and intercept parameter over the whole observation archive, based on

linear regression (LR). These parameters can then be used to tilt the backscatter distribution with respect to a certain reference incidence angle, which is generally chosen to minimise extrapolation errors. Regarding Sentinel-1, this estimation is more difficult due to a smaller range of incidence angles covered by the measurements resulting from the more stringent orbital configuration. Recent attempts have shown success when resampling Sentinel-1 data to 500 m and to estimate the slope parameter through a multivariate linear regression model (BAUER-MARSCHALLINGER et al. 2018). However, this approach could not been transferred to higher-resolution backscatter which is still an open research topic.

3 Region of Interest and Data Sets

The region of interest for this study covers the western part of North Tyrol and a small part of South Tyrol in the Austrian/Italian Alps. Based on the availability of snow profile and satellite data, the time span ranges from July 2015 to September 2017, thus comprising two winter seasons. The satellite data consists of Level-1 IW GRDH data from Sentinel-1A/B. It was preprocessed to get backscatter over ground (sigma nought, σ^0), and radiometric terrain flattened gamma backscatter (γ^0_{rtf}), which will be explained in more detail in the next chapter. Incidence angles data was also stored during the preprocessing routine to allow backscatter normalisation in downstream processing, which requires information about the topography and the observation geometry.
For two study years, approximately 300 manual snow profile measurements were provided by the *Lawinenwarndienst Tirol*, containing information about snow wetness, snow height, snow hardness, grain size, grain shape, grain type and snow temperature. Measurement locations usually vary, because the data collection is performed by different employees of *Lawinenwarndienst Tirol*, skiers or ski tourers on a voluntary basis. This leads to a broad distribution of data samples in space with the drawback of reducing the temporal comparability. Beside this data set, weather data from *Wetteronline.de* (i.e., rainfall and maximum temperatures) was also considered within our analysis.

4 Methodology

4.1 Radar Backscatter Normalisation

Radiometric terrain flattening is a relatively new approach to represent backscatter as γ^0, but additionally correcting for terrain, i.e. regions affected by foreshortening (SMALL 2011). SMALL'S (2011) method tries to resolve the one-to-many and many-to-one relationship between the slant and ground range geometry and gives preference to an estimate of the illuminated area instead of applying an incidence angle normalisation. The proposed algorithm starts by integrating the local illuminated area for each point on a DEM. This area is estimated in a plane perpendicular to the slant range, where overlapping regions (e.g., when foreshortening is present) sum up, thus yielding a better estimate of γ^0. Shadow regions are excluded and masked during this procedure as they do not contribute any information.
Radar backscatter normalisation with respect to the incidence angle is another way to account for the influence of terrain, and for some extent, also of land cover. Within the frame of this research, a focus was laid on two methods: linear regression and a novel approach, the Piecewise Linear Percentile Slope (PLPS) method.

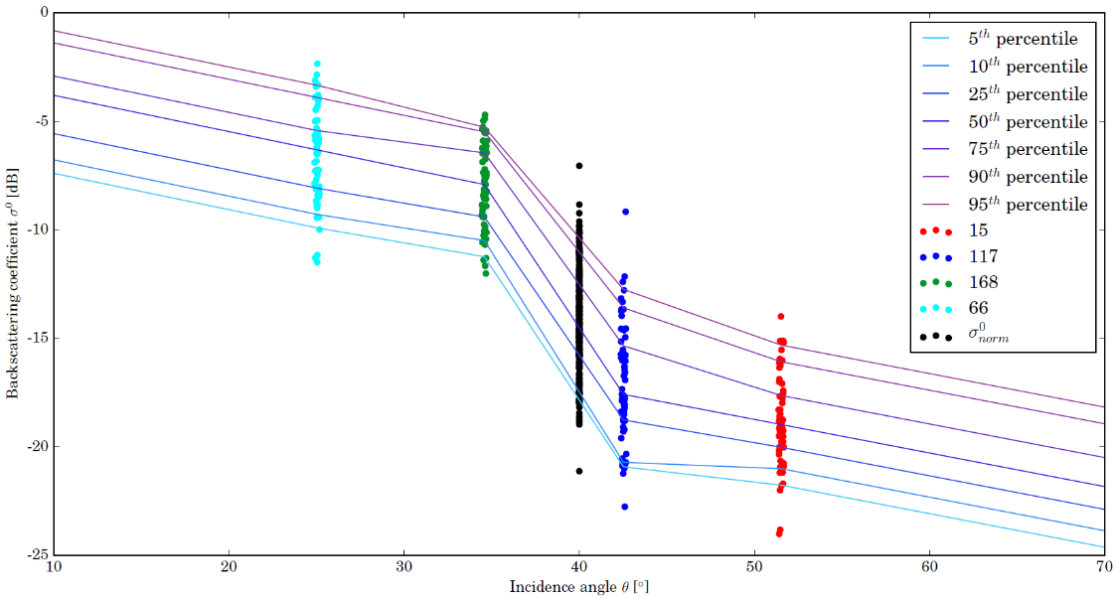

Fig. 2: PLPS normalised backscatter at a reference incidence angle of 40° (black) for a pixel located on a steep slope. Each point colour refers to a certain Sentinel-1 orbit and each line colour to a percentile

The idea of the here presented PLPS method is to discretise the backscatter distribution per orbit, instead of relying only on one single slope estimate for all orbits as it is the case for LR. Percentiles are thought to be the best choice for sampling the distribution, since they offer to derive a slope being dependent on the given backscatter distribution at a given incidence angle and are less influenced by outliers. However, a linear regression between equal percentiles and their related incidence angles does not work for a complex behaviour of backscatter, i.e. a non-linear behaviour along the range of incidence angles. This issue can be solved by going one step further in discretisation and connect each pair of percentiles between neighbouring orbits, which is depicted in Fig. 2. To minimise the necessity of extrapolation, 40° seems to be an appropriate choice for the reference incidence angle as the mean value of the Sentinel-1 incidence angles tends to be around 40°. For further analysis and comparison, σ^0 was once normalised with the LR method (σ^{40}_{LR}) and once with the PLPS method (σ^{40}_{PLPS}).

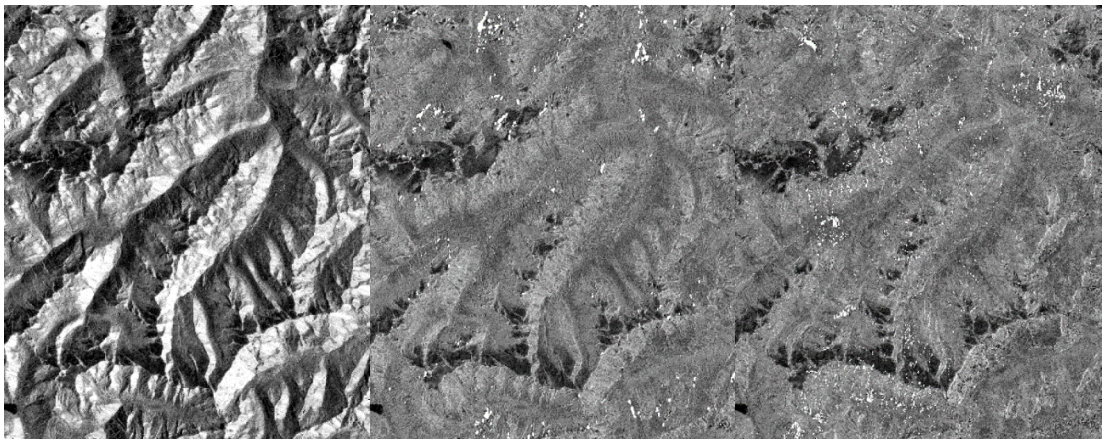

Fig. 3: Comparison between σ^0 (left), γ^0_{rtf} (center) and σ^{40}_{PLPS} (right).

Fig 3. underlines the capability of both radiometric terrain flattening and PLPS to reduce the impact of terrain on backscatter. In the left image, the typical illumination pattern of a SAR sensor is visible. Some regions appear very bright, because they are facing towards the sensor (foreshortening), while others are dark as they are situated on a slope turned away from the sensor. This behavior is very well compensated by means of backscatter normalisation as shown in the other two images. Shadow regions are masked for γ^0_{rtf}, whereas σ^{40}_{PLPS} excludes areas where no percentile slope estimation is possible, e.g., when only measurements from two orbits covering a small range of incidence angles are available.

4.2 Change Detection

Another way to deal with the influence of the observation geometry is to eliminate systematic effects by performing a subtraction between two backscatter values from the same orbit. By doing so, changes with respect to the chosen reference backscatter value can be detected and related to a geophysical variable, e.g., snow wetness. NAGLER & ROTT (2000) have used change detection for wet snow mapping relying on a selection of a suitable reference image (e.g., at dry-snow or snow-free conditions) to separate backscatter of a snow pack from surface backscatter.
The herein presented reference image selection follows recommendations of NAGLER & ROTT (2000) and NAGLER et al. (2016). In addition, the selection is explicitly assisted by continuously measured weather data. Past studies relied on a selection of one image, which is reasonable for a smaller test site. However, as this paper aims to compare backscatter measurements with snow profile data on a larger scale, a selection of a reference backscatter value is thought to be most reliable at pixel level, in contrast to image level. To detect the most appropriate backscatter values in a time series, meteorological data was interpolated at each pixel. Thereby, Inverse Distance Weighting (IWD) was applied for rainfall data and linear interpolation by height for temperature data. The final selection of a reference backscatter value is based on filtering the interpolated weather data in time, i.e. to find the pixel value with the coldest and driest conditions.

5 Results and Discussion

A subset of snow parameters was finally compared to the different backscatter representations, which are σ^0, γ^0_{rtf} σ^{40}_{LR} and σ^{40}_{PLPS}, for both polarisations VV and VH. From Fig. 4, one can conclude that normalised backscatter (lower rows) leads to superior results, with σ^{40}_{LR} performing best. This confirms the expectations of normalised backscatter not only being less dependent on terrain variations but also on the land cover type. Moreover, VH polarisation has a higher correlation for all snow parameters, which underlines the fact of multiple scattering and perhaps also the greater sensitivity with respect to fluid retention in a snow pack. Snow parameters such as air temperature, maximum snow wetness, mean grain size and mean snow wetness are characterised by a larger negative correlation, whereas snow height and the number of layers are positively correlated with backscatter.
However, one has to keep in mind, that there is a large inter-dependence between the individual snow parameters, and hence might influence the backscatter dynamics in a coupled way. This could be the case for snow parameters with a negative correlation, all thought to be dependent on snow wetness. In general, larger grains occur when the snow pack contains wet snow or is governed by past melt-freeze cycles. The same is true for air temperature with a maximum correlation

of -0.55: the warmer, the higher the probability of wet snow. A positive correlation with snow depth is meaningful (more volume scattering), but is not necessarily the only cause of the depicted correlations. It could be the case that the results are affected by the site and the land cover itself, i.e. the general level of the surface backscatter, because of the varying measurement location. Correlations shown in Fig. 4 are based on a single value retrieval, which is disturbed to some extent by speckle, noise or the snow profile measurement procedure, which impacts on the snow pack structure. Building a local average over a certain neighbourhood around the measurement site (around 30m) increased the correlations significantly. Furthermore, by applying change detection based on the generated reference image (referred to as backscattering difference), nearly all backscatter representations at VH polarisation reached a correlation of -0.64 with snow wetness. This behaviour is caused by the difference formation, where steady effects (e.g. terrain) cancel out (cf. Fig. 5, bottom).

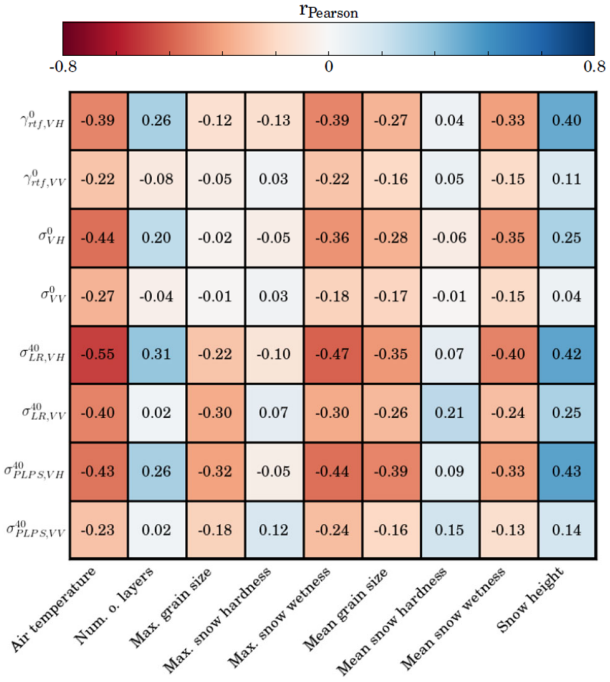

Fig. 4: Pearson's correlation coefficient resulting from relating backscatter to snow parameter data. Visual guidance is given through a colourisation of the correlation, where negative correlation is coloured as red and positive as blue

Fig. 5 depicts a time series of snow and C-band SAR backscatter parameters for a part of the winter season in 2017. One can identify the large variation of σ^0 caused by the different viewing geometries (Fig. 5, top). All other backscatter representations line up very well and confirm the success of each normalisation method. As mentioned before, the separation of all backscatter parameters is further reduced when applying change detection (Fig. 5, bottom). Both figures (Fig. 5 top and bottom) show a rather strong, positive correlation between air temperature and maximum snow wetness, with dominant peaks in March and April. They are delineated well by the troughs of the backscatter curves being even more distinctive for the backscattering differences. Applying a harsh threshold of -3 dB as proposed by NAGLER & ROTT (2000) would exclude some measured snow melt events. We therefore suggest to create a continuous classification of backscattering differences below 0 dB.

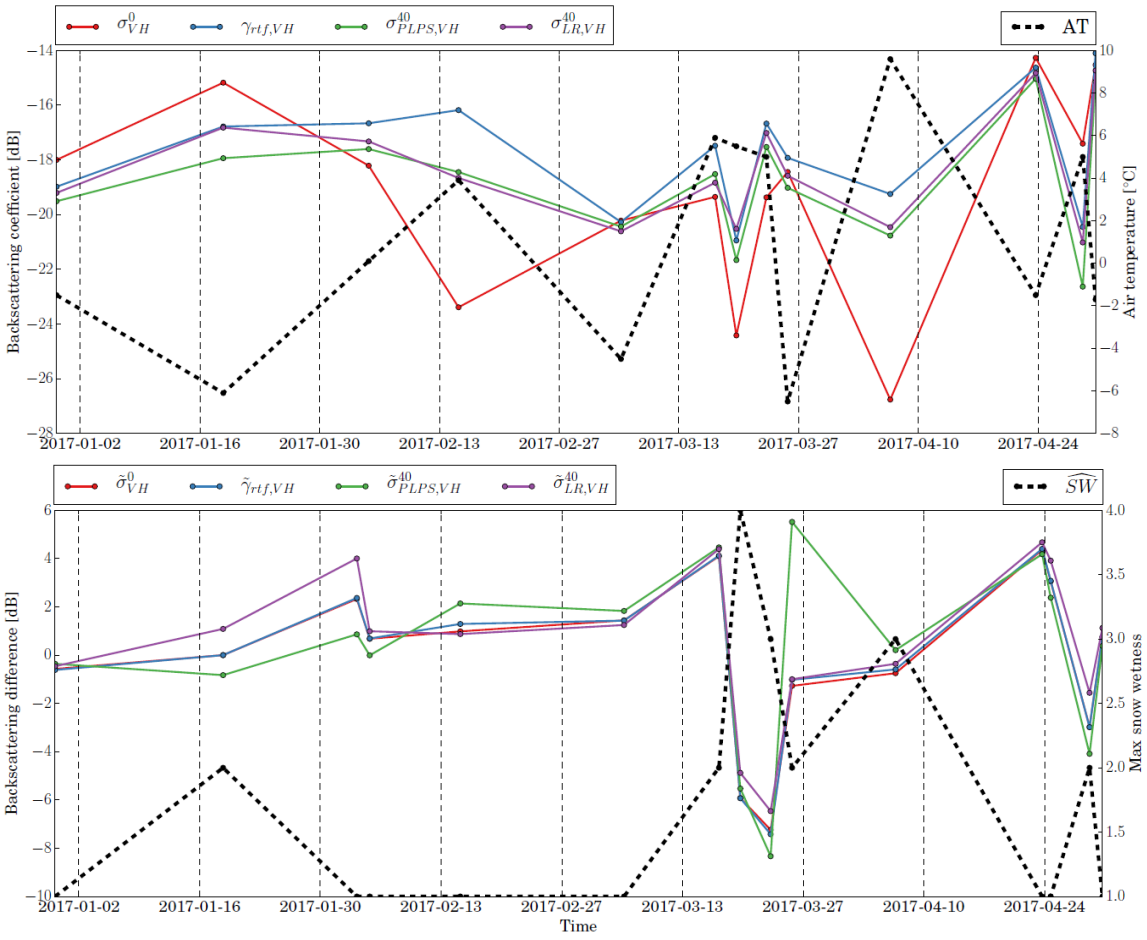

Fig. 5: Comparison between σ^0 (red), γ^0_{rtf} (blue), σ^{40}_{PLPS} (green), and σ^{40}_{LR} (violet) once for VH polarized backscatter and air temperature (top) and once for backscattering differences and maximum snow wetness (bottom), respectively

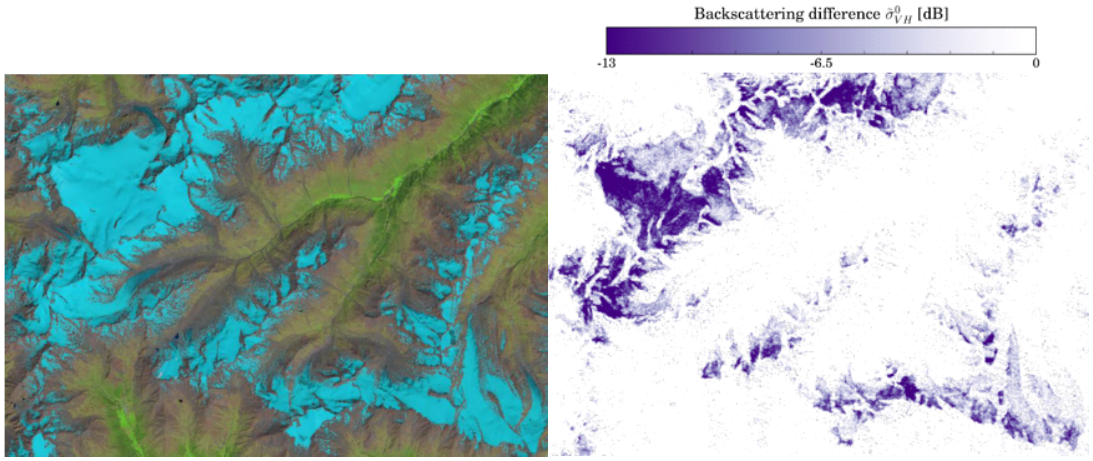

Fig. 6: Comparison between a Landsat 8 false-colour composite (left) and a map indicating wet snow (right)

The aforementioned findings can now be used to apply change detection on the backscatter data resulting in a map, which indicates snow wetness. In Fig. 6, such a map is compared to a Landsat 8 false-colour composite showing good agreement concerning the extent of the snow pack.

6 Conclusions and Outlook

In this study the relationship between the properties of alpine snow and C-band SAR backscatter observations from Sentinel-1 was investigated. To minimise the impacts of topography and imaging geometry, Sentinel-1 backscatter measurements were modified by means of radiometric normalisation, a novel incidence angle normalisation method and change detection. Correlations with snow parameters seem to be highest when applying a linear regression model, as it appears to be more robust concerning critical backscatter distributions at high and low incidence angles. Yet, the here presented piecewise linear percentile slope normalisation is considered to be superior if the Sentinel-1 orbits cover a broader range of incidence angles.
The results feature that Sentinel-1 backscatter shows the strongest (negative) correlation to manually measured snow wetness. The relation can be made even more pronounced by using change detection and spatial filtering (-0.64). Other snow parameters are also characterised by a high correlation, but being rather insignificant due to inter-dependencies and a varying land cover.
This work opens up further research questions, e.g., how to model additional orbit effects resulting from different viewing directions in azimuth or how to set up an objective snow parameter measurement configuration to reduce the influence of the surveyor.

7 References

BAUER-MARSCHALLINGER, B., FREEMAN, V., CAO S., PAULIK, C. SCHAUFLER, S., STACHL, T., MODANESI, S., MASSARI, C., CIABATTA, L., BROCCA L., WAGNER, W., 2018: Toward Global Soil Moisture Monitoring With Sentinel-1: Harnessing Assets and Overcoming Obstacles. IEEE Transactions on Geoscience and Remote Sensing, **99**, 1-20.

BERNIER, M. & FORTIN, J-P., 1998: The Potential of Times Series of C-Band SAR Data to Monitor Dry and Shallow Snow Cover. IEEE Transactions on Geoscience and Remote Sensing, **36.1**, 226-243.

MOREIRA, A., PRATS-IRAOLA, P., YOUNIS, M., KRIEGER, G., HAJNSEK, I. & PAPATHANASSIOU, K., 2013: A Tutorial on Synthetic Aperture Radar. IEEE Geoscience and remote sensing magazine, **1.1**, 6-43.

NAEIMI, V., SCIPAL, K., BARTALIS, Z., HASENAUER, S., & WAGNER, W., 2009: An Improved Soil Moisture Retrieval Algorithm for ERS and METOP Scatterometer Observations. IEEE Transactions on Geoscience and Remote Sensing, **47.7**, 1999-2013.

NAGLER, T. & ROTT, H., 2000: Retrieval of wet snow by means of multitemporal SAR data. IEEE Transactions on Geoscience and Remote Sensing, **38.2**, 754-765.

NAGLER, T., ROTT, H., RIPPER, E., BIPPUS, G., & HETZENECKER, M., 2016: Advancements for Snowmelt Monitoring by Means of Sentinel-1 SAR. Remote Sensing, **8.4**, 348.

POWER, D., YOUDEN, J., LANE, K., RANDELL, C. & FLETT, D., 2001: Iceberg detection capabilities of RADARSAT synthetic aperture radar. Canadian Journal of Remote Sensing, **27.5**, 476-486.

SHI, J. & DOZIER, J., 2000: Estimation of snow water equivalence using SIR-C/X-SAR: II. Inferring snow depth and particle size. IEEE Transactions on Geoscience and Remote Sensing, **38.6**, 2475-2488.

SMALL, D., 2011: Flattening Gamma: Radiometric Terrain Correction for SAR Imagery. IEEE Transactions on Geoscience and Remote Sensing, **49.8**, 3081-3093.